International Forum on Aeroelasticity and Structural Dynamics
IFASD 2017
25-28 June 2017, Como - Italy

INVESTIGATION OF FLUTTER CHARACTERISTICS OF AIRCRAFT WITH CONTROL SYSTEM

M. Zichenkov[1], A. Chizhov[1], S. Kuzmina[1], F. Ishmuratov[1], A. Zubakov[1]

[1] Central Aerohydrodynamic Institute named after prof. N.E. Zhukovsky (TsAGI),
Zhukovsky, Russia
stataer@tsagi.ru

Keywords: aeroelasticity, flutter, frequency response, control system.

Abstract: An effective method is developed for analyzing of flutter characteristics of the aircraft with control system taking into account unsteadiness of aerodynamic forces. The application of the method is demonstrated for typical examples of regional aircraft with engines under wing and maneuverable aircraft with container on the wing tip.

1 INTRODUCTION

Flight control system (FCS) of a modern aircraft is aimed to improve stability and controllability of rigid body motion of aircraft, and it responds to not only rigid body motion but also local elastic deformations of the structure near transducer position. The signals related with dynamic elastic deformations pass to executive controls of FCS due to high rate of actuators and cause additional perturbations both for rigid body motion and for elastic deformations. For this reason, the interaction between FCS operation and flutter characteristics can rise for modern aircraft.

A lot of scientific researches were dedicated to different aspects of aeroservoelasticity problems since the fifties of the last century; many of them are presented in [1-3]. Conditionally the researches can be divided into two groups. The first group of researches is dedicated to providing of dynamic stability in the interaction of elastic structure with regular FCS. The second extensive group of aeroservoelasticity researches is dedicated to study and application active control systems including flutter suppression systems.

The purpose of our work is development of an effective method of the analysis of flutter characteristics of aircraft with regular FCS taking into account unsteadiness of aerodynamic forces and demonstration of its application on typical examples.

According to standard practice in TsAGI and Russian aviation design bureau the researches of aircraft flutter and aeroelastic stability with FCS are performed by different expert groups using different methods. Flutter analysis is mainly based on the behavior of flutter equation roots, i.e. on the dependence of modal damping and frequencies on airspeed. Aeroelastic stability with FCS is mainly analyzed in terms of frequency response method (for example, using Nyquist diagrams).

Such division of researches exists also in regulated documents. For examples, Russian Aviation Regulations (item 25.629) assign to provide stability margins on structural and flow parameters for flutter investigation and to provide stability margins on amplitude (gain) and phase of open loop frequency response function (FRF) for aeroservoelastic stability. Approximately the same state is in other countries researches and regulated documents (FAR, MIL, CS etc.).

Flight dynamics of modern aircraft is inseparable from FCS operation. The analysis of tendency of aviation techniques development shows that the interaction between elastic structure and FCS increases for advanced aircraft. Therefore the adjustment of flutter stability margins on structural and flow parameters with aeroservoelastic stability margins is needed.

A large scope of researches is usually carried out for determination of characteristics of flutter and aeroservoelastic stability at aircraft certification. As a result, the availability of stability margins required by regulations is confirmed. The interaction of these phenomena is not usually investigated separately because of present regulations does not explicitly demand this.

But the analysis of flight test results of modern airplanes shows that considerable deflections of controls are often observed at high speeds and Mach numbers near expected flutter frequency. This may indicate a significant interaction of the flutter with the FCS operation. In this case it is important to study both the influence of FCS operation on flutter characteristics and the influence of the proximity of the flutter boundaries on aeroservoelastic stability margins.

For computation of aircraft flutter characteristics with unsteady aerodynamic forces usually the p-k method (or its modifications) [4-5], the g-method, etc. [6-7] are applied. For the flutter analysis with a control system it is not always possible to organize stable work of these methods because of the number of oscillatory and aperiodic roots of the closed-loop system "aircraft+FCS" varies with change of a flow speed, and iterations on frequency does not always converge.

For aeroservoelasticity problems the approach based on fractional-rational approximation of unsteady aerodynamic forces on reduced frequency is often used [8-9]. Such approach allows carrying out researches not only in frequency and root domain, but also in time domain, taking into account FCS operation. However, these approaches are connected with labour-consuming adjustment of approximation parameters for each configuration of the aircraft.

In this paper another approach is presented, which, in our opinion and experience, is effective and convenient for the analysis of aeroelasticity problems. Brief algorithms are presented in the section 2.

Two typical examples of the influence of FCS on flutter characteristics are considered in this study and the application of the developed method for investigation of this phenomenon is demonstrated. The interaction of elastic oscillations with FCS for regional aircraft with engines under wing is considered in section 3. FCS influence on flutter characteristics of the maneuverable aircraft with container on the wing tip is considered in section 4.

2 CALCULATION ALGORITHMS OF AN AIRCRAFT WITH FLIGHT CONTROL SYSTEM CHARACTERISTICS IN FREQUENCY, ROOT LOCUS AND TIME DOMAIN

It is assumed that vibration equations of the elastic airplane in airstream in frequency domain are written in the form:

$$\left(-\omega^2 C + j\omega D_0 + G\right) q = Q^a + R\delta_c, \tag{1}$$

where q is the vector of modal generalized coordinates; C, D_0, G are inertia, structural damping and stiffness matrices; δ_c is vector of control signals acting on actuators; R is transfer matrix.

For linear aerodynamics, the vector of generalized aerodynamic forces can be written in the form:

$$Q^a = -\left(\rho V j\,\omega D + \rho V^2 B\right) q + Q^w w \tag{2}$$

where ρ, V are airflow density and speed, $D=D(M, k)$, $B=B(M, k)$ – aerodynamic damping and stiffness matrices depended on Mach number M and reduced frequency $k=\omega{\cdot}b/V$ (b is reference chord), w is intensity of the air gust, Q^w is vector of wind gust efficiency.

It is assumed that the study of the aircraft flutter characteristics is performed and eigen modes set is chosen. It is usually enough to use 15-20 eigen modes for symmetrical case and 20-25 eigen modes for antisymmetric case for an airplane with a good analytical model to be sure that the probable flutter modes are not missed. A set of reduced frequencies is also determined (usually 5-7 values is enough). This number of reduced frequencies makes possible to represent the dependence of unsteady aerodynamic forces in the entire range of frequencies and velocities with sufficient accuracy. Calculations are performed for a number of values of the Mach number, which is the parameter of the equations. The validity of this approach is confirmed by the long-term practice of calculating studies of the aeroelasticity characteristics.

Equations (1) and (2) can be obtained in modal coordinates by using various mathematical models and software. In this paper we use a mathematical model based on Ritz polynomial method implemented in the ARGON software [10]. Unsteady aerodynamic forces are determined by the doublet lattice method (DLM).

For solving aeroservoelastic problems, the equations (1)-(2) are supplemented by the equations of FCS operation. Here the mathematical model of the FCS and the closed-loop system "aircraft + FCS" is used in the frame of software FRECAN developed for calculation and analysis of aeroservoelastic characteristics of aviation structures [11].

Experience shows that for the study of aeroelastic stability of an aircraft with FCS, the most convenient tool is the frequency response (FR) method. One of the advantages of this method is that FCS elements FR can be obtained independently of each other analytically or experimentally. In order to calculate unsteady aerodynamic forces in frequency domain correctly, the interpolation of elements of aerodynamic matrices on reduced frequency is performed.

In the analysis of time dependencies, it is assumed that nonlinearities can only be in the control system, and the structure and aerodynamic forces described by equations (1) - (2) are linear. Further a fractional-rational approximation is performed by a set of second order elements for the aircraft FR calculated taking into account the unsteady aerodynamic forces. Then, these elements and nonlinear FCS elements are used in the formation of time-domain equations for specific selected input-output combinations. Unsteady aerodynamic forces and nonlinearities in the control system are correctly taken into account within made assumptions.

For a more complete and comprehensive study of stability margin in terms of flow parameters, structure parameters and FCS parameters, calculation and analysis of locus-root is also required. To determine the roots of the closed-loop system "aircraft + FCS", an algorithm based on the preliminary calculation of a dependence of roots on reduced frequency is used. It consists of the following steps:

- The parameter P is selected. Stability limits and margins are determined in terms of *P*. Usually it is an airflow speed or a density, or the FCS parameter (for example, the gain of the channel).
- For the selected parameter values, the roots of the closed-loop system $\lambda_i(P,k) = \delta_i(P,k) + j\omega_i(P,k)$ are computed. This calculation is carrying out for a given number of the reduced frequency *k* values and the dependence $\omega_i(k)$ is determined.
- The equation $\omega_i(P,k) = kV/b$ is then numerically solved using linear interpolation (notice that in the $p-k$ algorithm [4, 5] this equation is usually solved by a simple iteration method, which does not converge sometimes). The damping $\delta_i(P,k)$ and frequency $\omega_i(P,k)$ from the solution of the equation are used to plot dependencies of the roots on the selected parameter.
- This procedure is repeated for all parameter values and for all roots. Dependencies *V-g Plot*, *V-f Plot* are obtained and as the result the parameter stability boundary and the oscillation frequency are determined.

The obvious drawback of the algorithm is that the calculations effort (the solution of eigenvalue problem) is much greater versus a simple iteration. However, this drawback is compensated by the stable algorithm operation, and some slowing down of calculations is almost imperceptible in modern computers.

It should be noted that the oscillation frequencies $\omega_i(P,k)$ dependence on the reduced frequency *k* for different values of the parameter *P* can have varying shape. Because of this, the number of solutions (roots) can be different. For example, such dependencies for two modes of oscillations of a maneuverable aircraft are shown in figure 1 and figure 2. In the first case, just one root is obtained for the simple mode shape of horizontal tail. In the second case, a complex mode shape (torsion of the fuselage with bending and torsion of the wing and tail, figure 3) causes a complex dependence $\omega_i(P,k)$, as a result, three roots are obtained. The appearance of additional roots is associated with the flow dynamics due to the unsteady aerodynamic forces. As a result, complex dependencies of frequencies and damping to the parameter can be obtained, as shown in figure 4 (fragment). The developed calculation algorithm is stable at analyzing such cases.

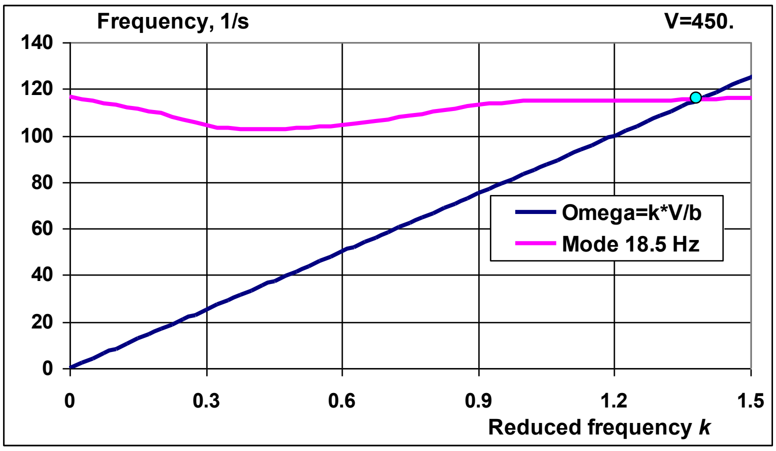

Figure 1: Frequency for mode "18.5Hz" versus reduced frequency (*V*=450m/s)

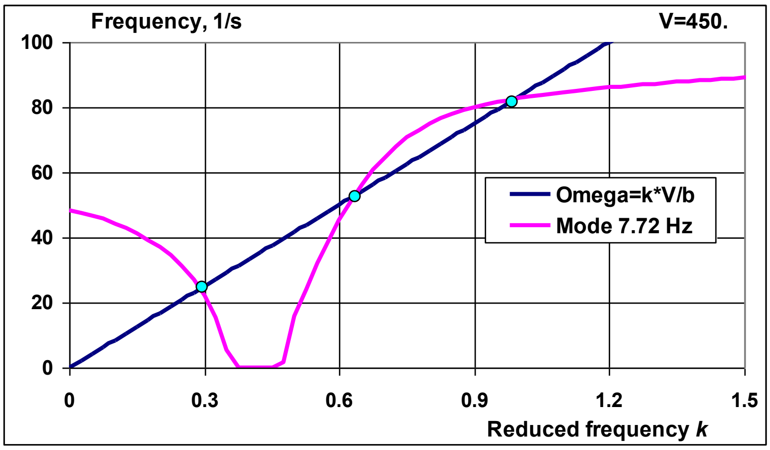

Figure 2: Frequency for mode "7.72Hz" versus reduced frequency (*V*=450m/s)

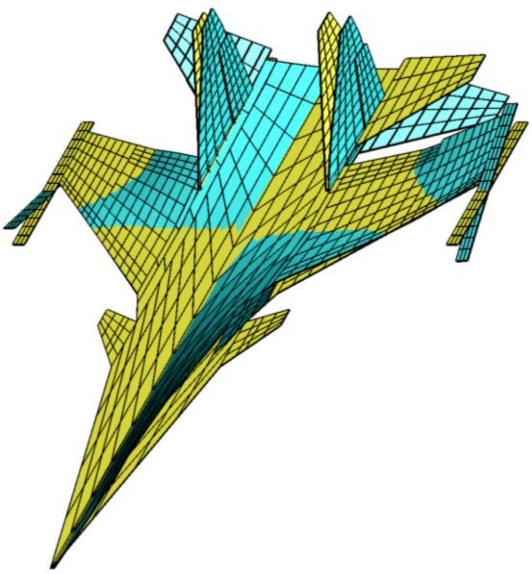

Figure 3: Mode shape "7.72 Hz"

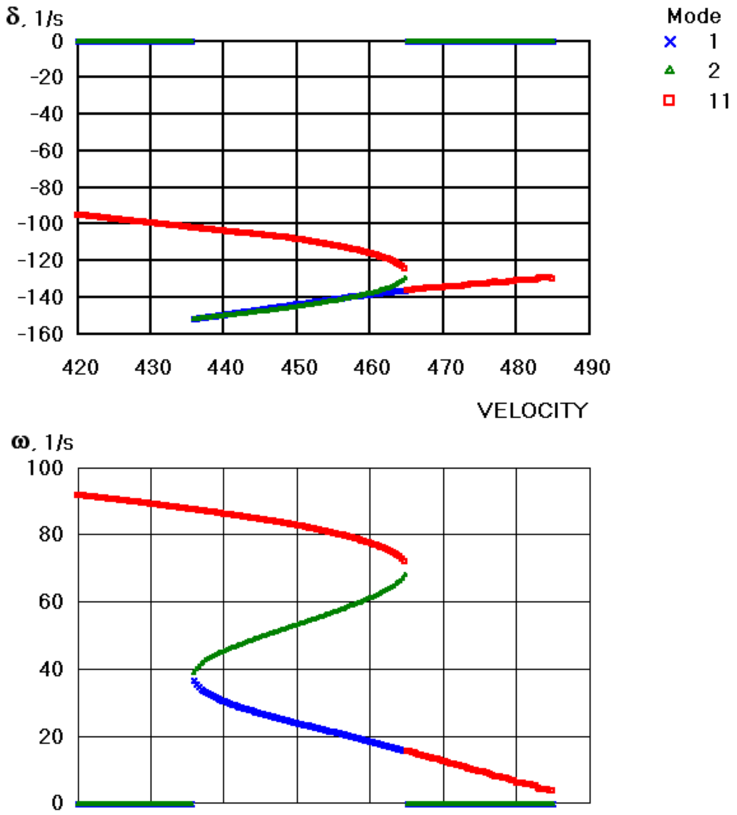

Figure 4: Damping and oscillation frequency for eigen mode "7.72Hz" versus airspeed (fragment)

3 AEROSERVOELECTRIC STABILITY ANALYSIS OF A REGIONAL AIRCRAFT WITH A FLIGHT CONTROL SYSTEM

In this section, the interaction of the flutter characteristics with flight control system (FCS) is studied for the regional aircraft (RA) computational model (figure 5). The ARGON software mathematical model of the aircraft and the FRECAN software mathematical model of the FCS longitudinal channel are used.

Unsteady aerodynamic forces are calculated by doublet lattice method (DLM). The elastic-mass properties of the structure are described by Ritz polynomial method in the beam approximation. The total mass of the aircraft is about 25 tons.

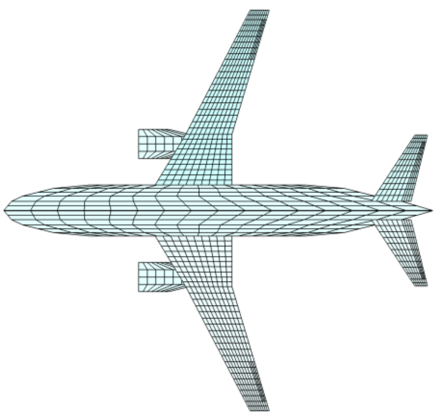

Figure 5: Aerodynamic model of the RA

3.1 Flutter characteristics

Below the results of flutter studies of the aircraft are summarized. The results were obtained within ARGON software:

- The determining flutter mode is the symmetrical flutter for minimum weight at high altitudes. This flutter mode is represented by pitching oscillations of the engine and the wing bending oscillation.
- The flutter frequency is about 5Hz and its equivalence airspeed is in the range 700÷800 km/h. As the speed increases, the aircraft is out of flutter.
- The second mode of flutter with a frequency of about 8 Hz is represented by bending-torsional oscillations of the wing tip. This flutter occurs at 1100-1200 km/h.
- Characteristics of the first flutter mode ("5 Hz") depend on various structure and air flow parameters: aircraft weight, flight altitude, Mach number, unsteady aerodynamic forces consideration at alias.
- Correct consideration of unsteady aerodynamic forces is important in the analysis of this flutter mode. For example, when using the quasi-steady aerodynamics, a flutter with a frequency of about 17.5 Hz appears in the computational model. For a small fixed reduced frequency, the dependence of the frequencies and decrements of the oscillations on the flow velocity also differs significantly.
- A noticeable effect on the flutter mode decrement and the flutter speed is exerted by the balance at the wing tip. The flutter-preventive weight of 20 kg, located approximately along the axis of stiffness at the end of the wing, increases the flutter speed by 8%.

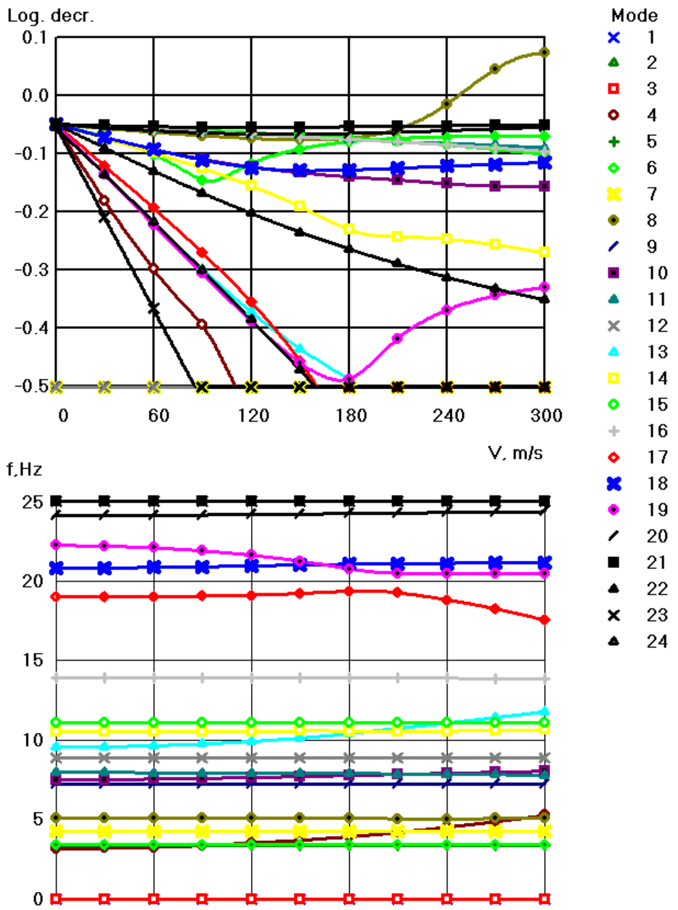

Figure 6: V_{fl}=250 m/s EAS, f=5.03 Hz (G=25 tons, H=4000 m, M=0.77)

3.2 Frequency response of the aircraft without FSC

In this section the pitching motion with symmetric elastic oscillations is considered. The flight control system uses the signals of normal acceleration and pitch rate transducers. The control surface is the elevator. The transducers of the inertial reference system (IRS) are located in the forward part of the fuselage. Two eigen modes are of interest from the point of view of FRF in longitude channel: engine pitch oscillations with a frequency of 5.0 Hz and vertical bending of the fuselage with a frequency of 7.5 Hz. These two modes are shown in figures 7, 8. The position of the transducers is also presented. Notice that both normal acceleration and angular rate transducers should have noticeable responses nearby the frequencies range of the modes mentioned above.

The aircraft frequency response due to the elevator harmonic deflection for several airspeeds up to the flutter speed is shown in figure 9. As far as the airspeed reaches the flutter speed (true speed at 4 km $V_{fl} = 250$ m/s), the frequency response extreme at the engine pitch oscillations frequency increases sharply. This should lead to the change in flutter characteristics of the closed-loop system.

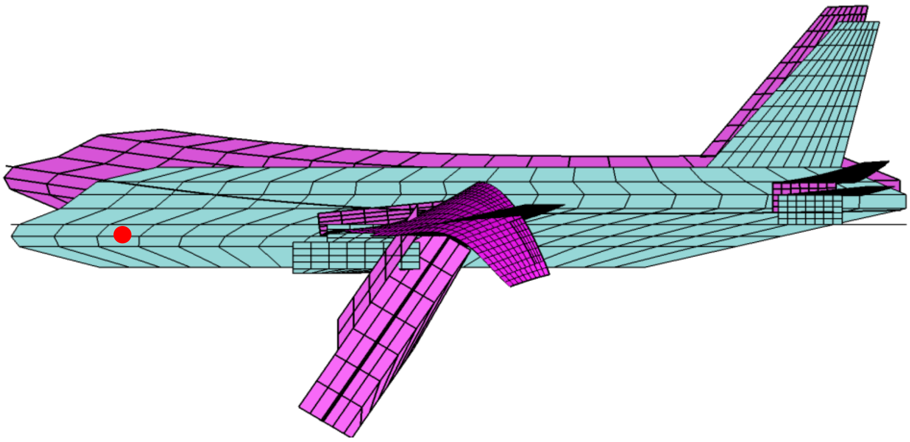

Figure 7: Engine pitch oscillation mode (*f*=5.0 Hz)
● - IRS position

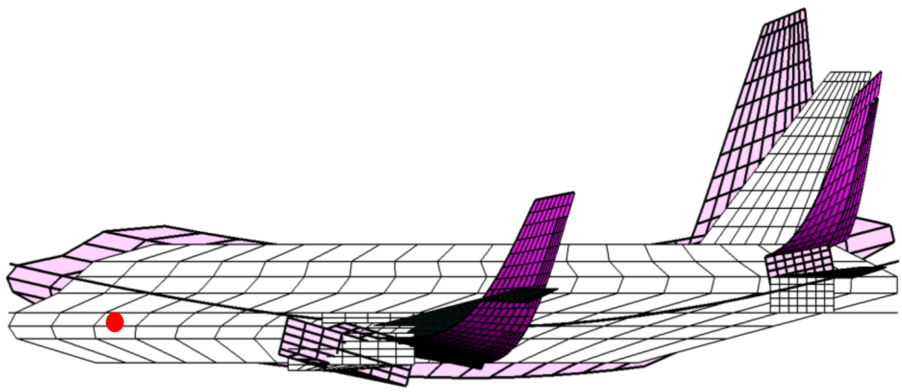

Figure 8: Fuselage vertical bending oscillation mode (*f*=7.50 Hz)

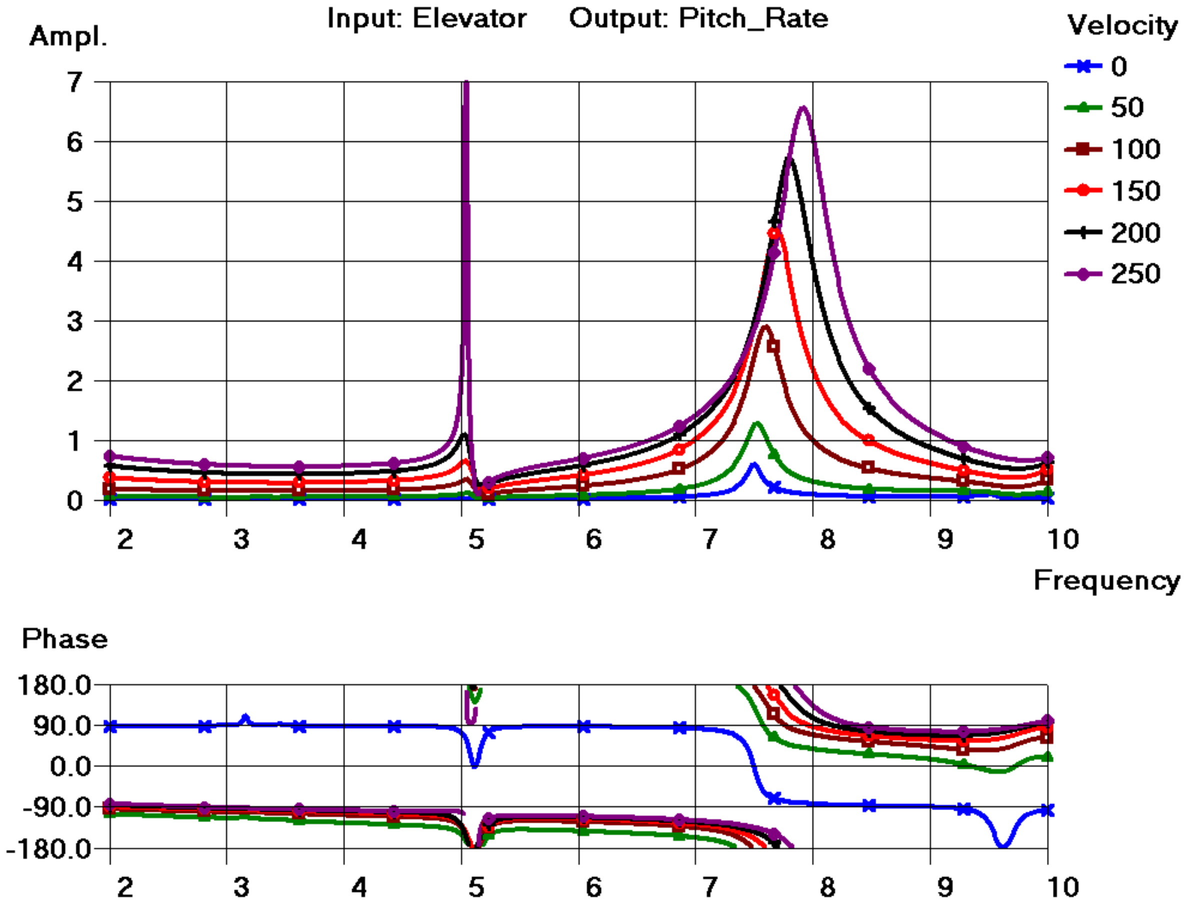

Figure 9: Frequency response of pitch angular rate to harmonic elevator deviations

3.3 Frequency response the aircraft with FCS

The structural flow chart and parameters of a simplified pitch channel of the FCS are shown in figure 10. The signals of normal load factor transducer and pitch rate transducer are fed to the elevator drive through the appropriate filters and coefficients of the control system. The amplifying coefficients depend on Mach number and velocity. The coefficients are taken for the maximum speed for Mach number M=0.77; they were assumed to be constant.

To analyze the aeroelastic stability of the airplane with the FCS, the FRF of the open-loop system was calculated. The signal ratio U_{fb} / U_{inp} at K = 0 was analyzed (see figure 10). For calculations FRECAN software was used.

The analysis of the frequency response in the form of the Nyquist diagram (see figure 11) shows that the FCS has a destabilizing effect on the aircraft in frequency range near 5 Hz. When speed is above 237 m/s, but less than the flutter speed (V_{fl} =250 m/s), the Nyquist diagram envelope the point (+1, 0j), which indicates a loss of stability of the closed-loop system. Such an effect of the FCS on the flutter characteristics is due to the signal of the pitch rate channel.

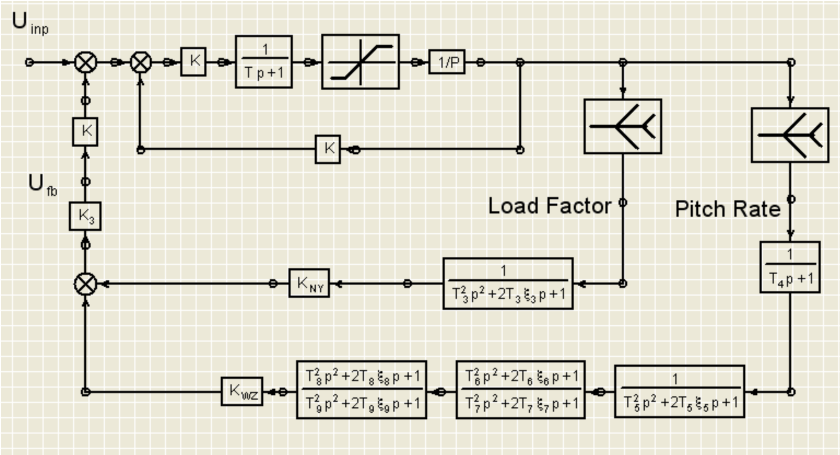

Figure 10: Block-diagram of simplified longitudinal channel of FCS

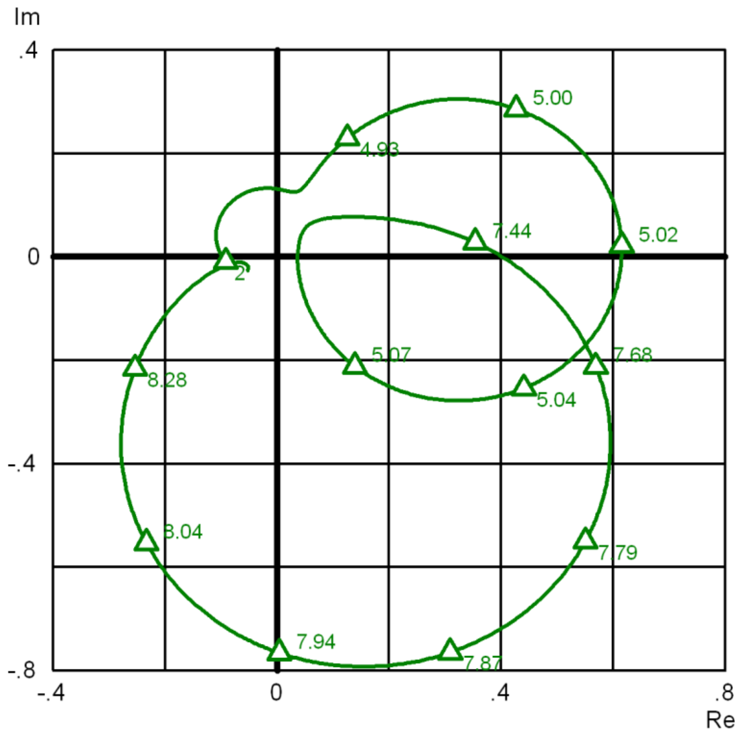

Figure 11: "Aircraft+FCS" Nyquist plot for U_{fb}/δ_{inp} (V=230m/s)

3.4 Oscillation frequencies and decrements of the aircraft with FCS

As shown above, the influence of the FCS on the flutter boundaries can be investigated by the open-loop Nyquist plot. But this approach is not convenient for parametric studies. For a linear system, the effect of the FCS on the flutter characteristics can be more clearly illustrated by the root locus of a closed-loop system. For this purpose, FRECAN software with the aircraft and FCS models described above was used.

Figure 12 shows frequencies and damping coefficients of aircraft oscillations with the FCS as a function of velocity. The flutter starts at speed less than speed V_{fl} obtained for the airplane without FCS (see figure 6). This agrees with the above analysis of the open-loop system.

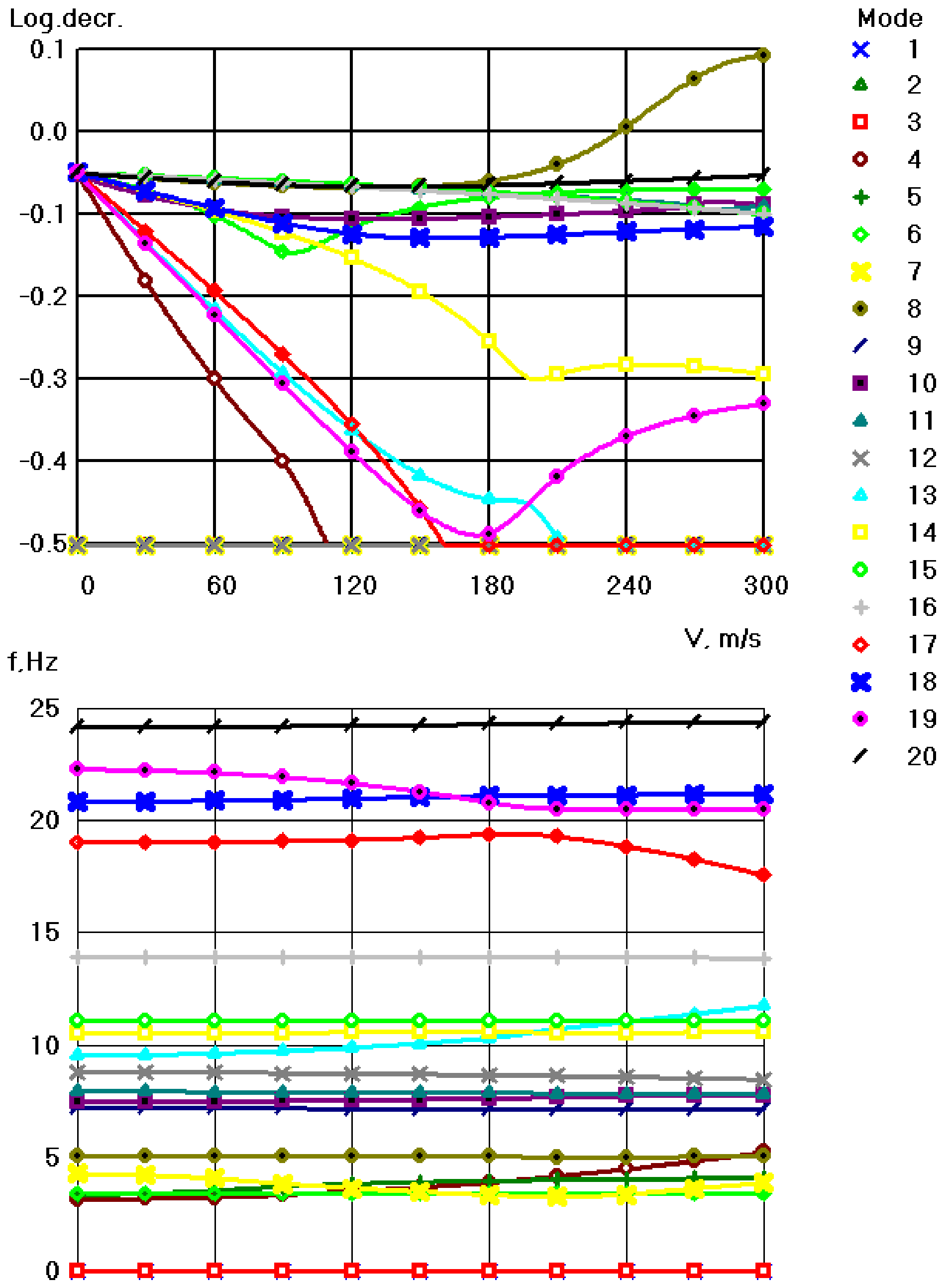

Figure 12: Oscillation damping and frequencies of the aircraft with FCS to velocity (V_{fl}=237 m/s, f=5.03 Hz)

Notice that calculations of the aircraft model and the FCS correspond to the high velocities regime, and therefore the damping characteristics for small and moderate velocities are determined approximately.

The effect of the FCS on the flutter characteristics is shown in figure 13. In the figure comparison of the flutter mode logarithmic decrement for the aircraft without the FCS and with the FCS one is shown. The comparison shows that the operation of the FCS reduces the flutter mode decrement by approximately 0.01-0.02 at the high-speed range. The flutter speed reduction may have various types, depending on the decrement-velocity relation. For the model concerned, the decrease in the flutter velocity is about 5%.

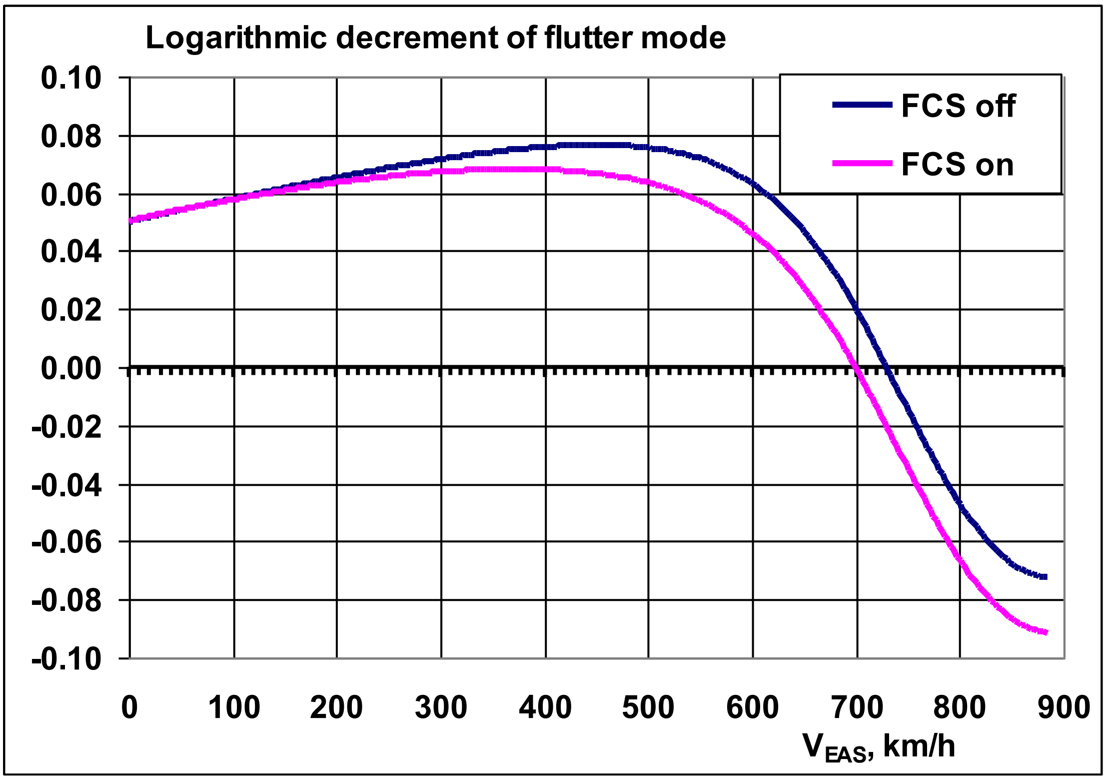

Figure 13: Flutter mode decrements comparison

3.5 Dynamic response of the aircraft with FCS in time domain

To complete the studies of the interaction of the structure elastic deformations, calculations in time domain are also performed. The impact of a single impulse with a profile is considered:

$$w = 0.5 w_0 (1 - \cos(2\pi x / L))$$

The wavelength L = 50 m and intensity w_0 = 15 m/s are chosen from the condition of maximum excitation of flutter oscillations.

Analysis of time processes shows that the aircraft is stable in the flutter speed range. But the slightly damped engine pitch oscillation mode with a frequency of 5 Hz is strongly appear at all parameters. At airflow speed 240 m/s, closed to the stability boundary, steady-state oscillations are observed. These oscillations correspond to the rudder deflection of 0.5-0.6 degrees. Comparison of the aircraft response to the elevator deflection, normal acceleration and angular pitch rate for the aircraft without the FCS and with the FCS one at a speed of 245 m/s is shown in figure 14. For the aircraft with the FCS, a significant amplitude increase of the oscillations is observed.

With a further increase in air speed (figure 15), with the same disturbance, in closed-loop system self-oscillations occur. Amplitude of this oscillations correspond to the amplitude of the elevator oscillations about 1 degree. The amplitude of self-oscillations is determined by the limitation of the actuator rate (30 degrees per second, see figure 10).

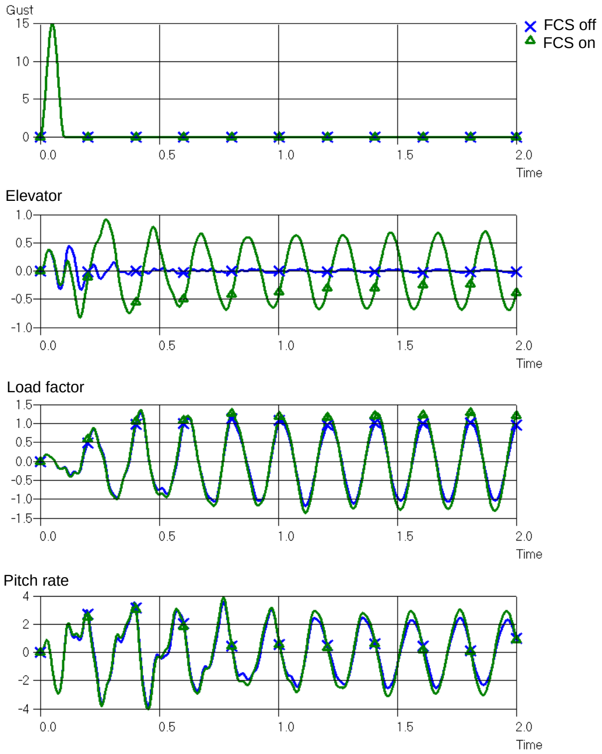

Figure 14: Wing gust response for the aircraft without FCS (blue line) and the aircraft with FCS (green line) V=245 m/s

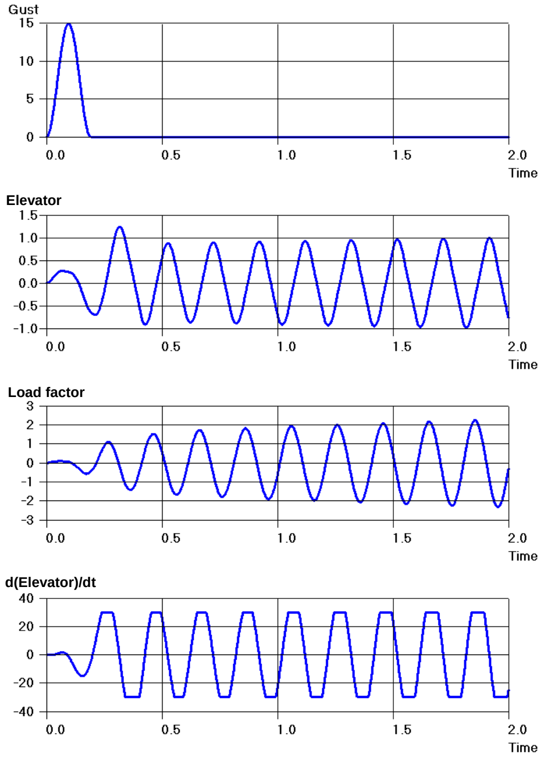

Figure 15: Wing gust response for the aircraft with FCS (V=260 m/s)

The performed researches showed:

- In the high-speed range, closed to the flutter velocity, the FCS has the destabilizing effect near the flutter mode frequency.
- Root locus analysis of the linearized closed-loop system shows that in the high-speed range the FCS operation reduces the logarithmic decrement of the flutter mode by approximately 0.01-0.02. The decrease in the flutter speed is about 5%.

4 ANALYSIS OF AEROELASTIC STABILITY OF A MANEUVERABLE AIRCRAFT

Influence of flight control system (FCS) on flutter characteristics of the maneuverable airplane is considered. The mathematical model of the aircraft is created in ARGON software. The design scheme of the aircraft was verified by comparison of the calculated frequency response and experimental data.

For the analysis of the airplane with FCS in the roll channel, in the mathematical model of the control system channels from the roll and yaw angular rate transducers and lateral acceleration transducer were kept. These transducers could have a significant influence in aeroelastic stability frequency range of the aircraft in roll channel. Calculations of stability characteristics of the aircraft with the FCS were carried out in FRECAN software [5] in frequency, time and root domains. The block-diagram of the control system is shown in figure 16. Actuators are modeled by linear filter of the second order.

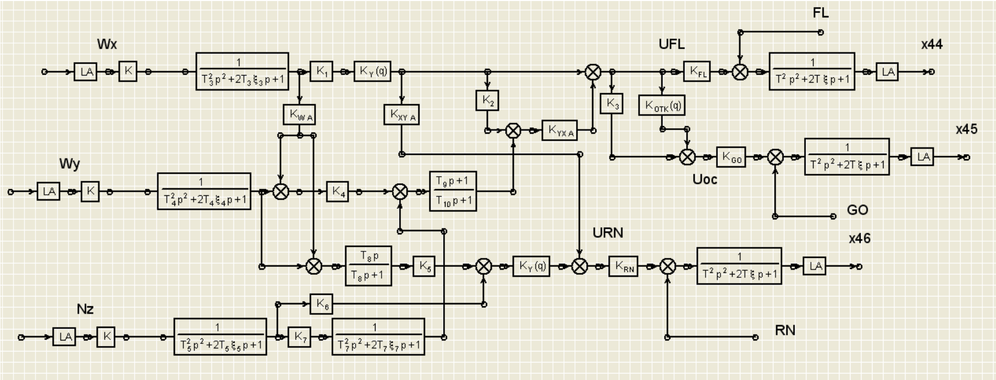

Figure 16: Block-diagram of the FCS roll channel

4.1 Aircraft and FCS aeroelastic interaction

Without FCS, an antisymmetric bending-torsion flutter of the wing with a container at wing tip (figure 17) occurs at speed $\overline{V}_{fl} = 1.17$ with a frequency f = 4.66 Hz (figure 18). An analysis of the flutter mode shows that the wing oscillations are accompanied by significant antisymmetric oscillations of the horizontal tail (H-tail). Therefore, it can be assumed that when the FCS is on, the oscillations of the H-tail can excite or damp oscillations of the whole aircraft at the flutter frequency, depending on the tuning of the FCS algorithms.

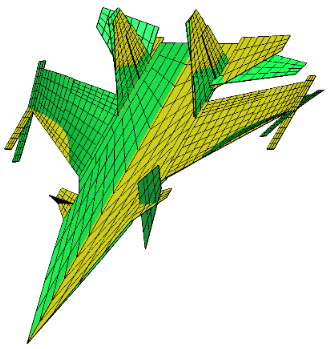

Figure 17: Flutter mode

Another viewpoint of the same phenomenon consists in analyzing of the aircraft amplitude-phase frequency response of the antisymmetric wing oscillations to the roll rate (Figure 19). Flight speed increase leads to increase of roll angular velocity transducer response at a frequency of 4.6 Hz. This can cause aeroelastic interaction with the FCS. Time dependencies (Figure 20) confirm the presence of undamped oscillations in a closed loop.

Calculation of the amplitude-phase-frequency characteristic of the "aircraft+FCS" system shows that switching on of the FCS leads to loss of aeroelastic stability ($\overline{V}_{fl} = 0.99$, f = 4.64Hz). Notice that flutter velocity is greater by almost 20% when the channel $U_{\text{HT}} / \delta_{\text{HT}}$ is open (figure 16).

Parametric velocity calculation of the flutter damping and frequency of open- and closed-loop system shows that the logarithmic decrement in open-loop is greater by 0.05 than closed-loop one. Unacceptably low damping is observed in a wide speed range.

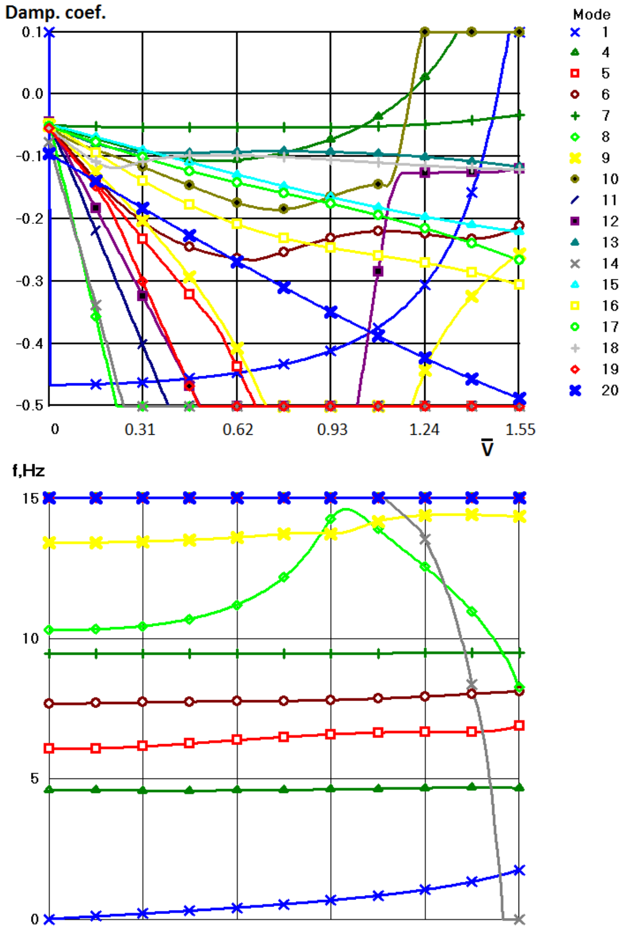

Figure 18: Oscillation damping and frequencies versus relative flight speed

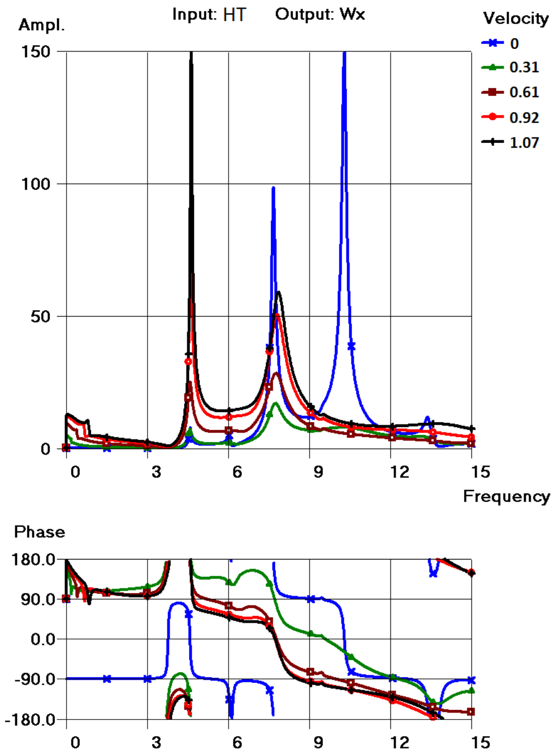

Figure 19: Frequency response ω_x/δ_{HT} for several airspeed

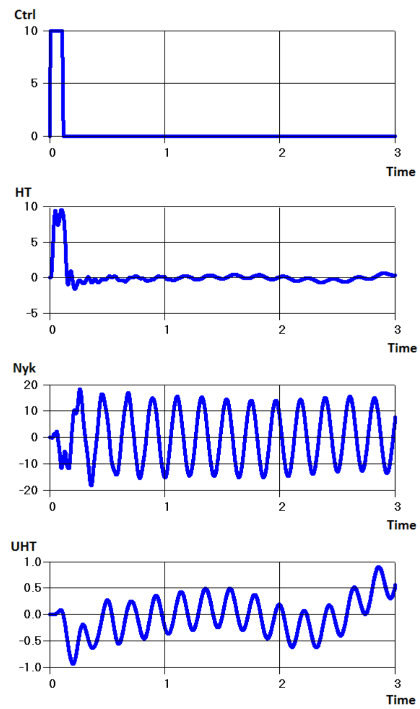

Figure 20: Roll channel impulse time response, closed-loop, $\overline{V} = 1$

4.2 Frequencies and decrements of the aircraft with a FCS

On the basis of the models described above, parametric calculations of the aircraft-FCS system decrement and oscillation frequencies for several flight regimes were carried out. All calculations were carried out for the antisymmetric case for the corresponding parameters: density, sound velocity and Mach number.

Figure 21 shows the dependence of the decrement and the frequency versus the relative flight speed which was obtained by calculation for height *H*=1000m. Also flight experimental results for the configuration under study. Notice significant influence of the control system on the flutter logarithmic decrement. Decrement decreases by 0.05 because of FCS operation.

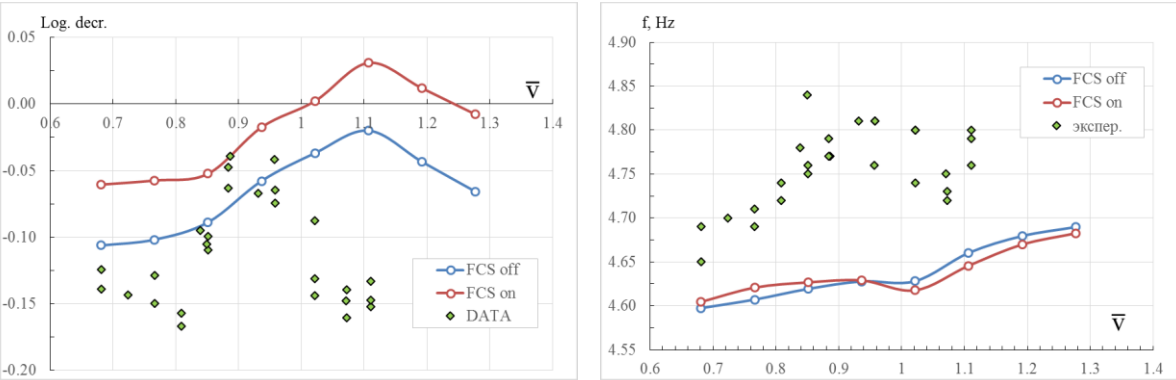

Figure 21: FCS effect on the dependence of flutter logarithmic decrement and frequency. Comparison with experimental data

In the experiment, from the speed $\overline{V} = 0.85$ there is a abrupt decrease in the damping. Minimum of the decrement is reached in the range. Calculation also shows a decrease in the damping of the structural oscillations, however, the minimum is achieved near $\overline{V} \approx 1.15$ and does not have such a pronounced gradient. The difference in the dependence of the decrement in calculations and experiment can be explained by transonic effects (the motion of shock waves), which were not taken into account in the calculation. Change of the oscillation frequency is more smooth. In the experiment the frequency is a little higher (from 1% to 4%).

4.3 FCS parameters changing and an increase of the stability margin for flutter velocity

The above computational studies of the aeroelastic stability of the aircraft with FCS have shown the poor of margins of aeroelastic stability in the roll channel in the range of transonic flight regimes at low altitudes. The results of the calculations are in good agreement with the flutter flight test data.

A lot of parametric calculations for the FCS modification has been carried out to increase the aeroelastic stability margin. As a result of the research, two variants of an additional elastic oscillation filter (EOF) for elastic oscillations in the roll channel were chosen:

$$EOF\_1 = \frac{T_1^2 p^2 + 2\xi_1 T_1 p + 1}{T_2^2 p^2 + 2\xi_2 T_2 p + 1} \quad T_1 = 0.03\text{s}, \quad \xi_1 = 0.1, \quad T_2 = 0.04\text{s}, \quad \xi_2 = 0.5$$

$$EOF\_2=\frac{T_1^2p^2+2\xi_1T_1p+1}{T_2^2p^2+2\xi_2T_2p+1}\times\frac{1}{T_3p+1}\quad T_1=0.016s,\ \xi_1=0.2,\ T_2=0.041s,\ \xi_2=0.5,\ T_3=0.05s$$

The additional filter is installed in series with a regular filter EOF.

For first additional filter EOF_1, the amplitude of U_{HT} / HT for the open loop is reduced to the value $\bar{A}=0.173$ at the flutter frequency. The phase is close to -90° (figure 22). The flutter speed of the closed-loop system is close to the flutter speed of an airplane without the FCS (figure 23).

For second variant of the filter EOF_2, the amplitude of U_{HT}/HT for the open loop is reduced to the value $\bar{A}=0.3$ and the phase is close to 180°. In this case FCS has a damping effect on the flutter oscillations (figure 22). Flutter speed of the closed-loop system is higher than the speed of the flutter of the aircraft without a FCS (figure 23). If necessary, it is possible to increase the flutter speed of the closed-loop system "aircraft + FCS" to the value $\bar{V}_{fl}\geq 1.2$. To this effect it is needed to configure the parameters of the additional filter by flight regimes.

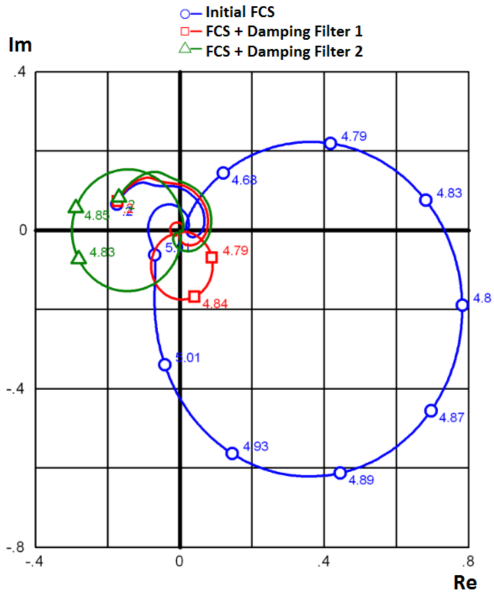

Figure 22: Nyquist diagram of the U_{HT}/HT channel of the open-loop system

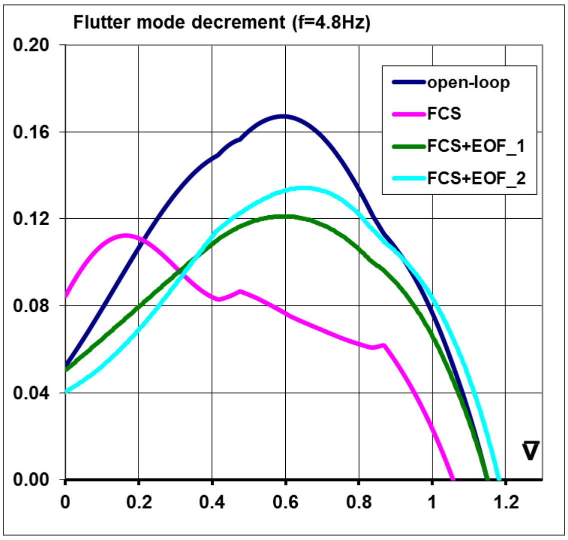

Figure 23: Flutter mode decrement

Thus, for the mathematical model of a maneuverable airplane with, the aeroelastic interaction of the aircraft and the FCS in is considered. This interaction is explained from different points of view. It is shown that the main reason of stability loss is due to the interaction of the signal of the FCS transducer with the wing bending-torsional oscillations and differential horizontal tail deviations.

It is shown that the FCS decrease logarithmic decrement by about 0.05 and decrease, and the flutter speed by 16-18%. So aeroelastic stability margin becomes insufficient at transonic flight regimes.

To increase the aeroelastic stability margin, it is proposed to modify the FCS elastic filter in the roll channel. It is shown that the modifications provide aeroelastic stability margin with the FCS and increase the flutter speed for the closed-loop system.

5 CONCLUSION

The method of flutter characteristics analysis taking into account the unsteadiness of the aerodynamic forces, described above, for an aircraft with a control system, is intended for practical use. It was demonstrated effectiveness of the method for assessing the effect of a flight control system on the characteristics of a flutter for two cases: for the passenger aircraft with engines under the large aspect ratio wing and for the maneuverable aircraft with containers at the wing tip. The results of the research accentuate the need for a deeper coupled study of the flutter characteristics and aeroelastic interaction of the aircraft with the FCS.

6 REFERENCES

[1] J.R. Wright and J.E. Cooper, Introduction to Aircraft Aeroelasticity and Loads, John Wiley, 2007

[2] Ashish Tewari. Aeroservoelasticity: Modeling and Control (Control Engineering). Springer, 2015, 318 p.

[3] Giulio Romanelli. Computational Aeroservoelasticity of Free-Flying Deformable Aircraft. PhD Thesis, Politecnico di Milano. March 2012.

[4] Rodden, W.P., and Johnson, E.H., MSC/NASTRAN Aeroelastic Analysis User's Guide, Ver.68, MacNeal-Schwendler, LosAngeles, CA,1994

[5] Rodden W.P. Theoretical and Computational Aeroelasticity. Crest Publishing, USA, 2011. ISBN 0692012419

[6] Chen, P. C., "Damping perturbation method for flutter solution: the g-method," AIAA Journal, Vol.38, No.9, 2000, pp. 1519-1524.

[7] Gu Yingsong, Yang Zhichun, Wang Wei, and Xia Wie. Dynamic Pressure Perturbation Method for Flutter Solution: the Mu-Omega Method. AIAA 2009-2312

[8] Roger, K. L., "Airplane Math Modeling and Active Aeroelastic Control Design," AGARD-CP-228, 1977, pp. 4.1- 4.11.

[9] Karpel, M., "Design for Active Flutter Suppression and Gust Alleviation using State-space Aeroelastic Modeling," Journal of Aircraft, 1982, Vol. 19, No. 3, pp. 221-227

[10] Ishmuratov F.Z., Chedrik V.V. ARGON Code: Structural Aeroelastic Analysis and Optimization. In: International Forum on Aeroelasticity and Structural Dynamics (IFASD), Amsterdam, 2003.

[11] Zubakov A.V., Zubakova O.V., Ishmuratov F.Z., Timokhin V.P. Software package FRECAN for calculating and analyzing aeroservoelasticity characteristics of aviation structures. The certificate of state registration No 2015610225, October 2014.

COPYRIGHT STATEMENT